Bull. Mater. Sci., Vol. 17, No. 6, November 1994, pp. 1039–1047. © Printed in India.

Growth, characterization and electrical anisotropy in GaTe—a natural semiconducting superlattice

S PAL and D N BOSE
Materials Science Centre, Indian Institute of Technology, Kharagpur 721 302, India

Abstract. GaTe is a III–VI semiconductor which has layered structure with large anisotropy in electrical properties. Growth of single crystals by the Bridgman technique permitted the measurement of thermoelectric power in orthogonal directions from which the anisotropy of hole effective masses were determined for the first time. From resistivity and Hall effect measurements the carrier activation energies and scattering mechanisms between 10–300°K were found.

Study of the temperature dependence of conductivity revealed a variety of conduction mechanisms including weak localization below 20°K, hopping conduction between 20–50 K and band conduction in and across the layer planes at $T > 70$ K. Weak localization was confirmed through observation of negative magnetoresistance. The *I–V* characteristics showed quantized behaviour due to tunneling across potential barriers, which may be due to stacking faults between layer planes as observed by TEM studies.

Keywords. GaTe; III–VI semiconductor; electrical anisotropy.

1. Introduction

GaTe crystallizes in the monoclinic system (space group C_2^2). According to the Mooser–Pearson criterion it is a III–VI semiconductor having one cation–cation (M–M) bond and forms X–M–M–X chains. There is strong covalent bonding within the layer planes with weak van der Waals bonding between them resulting in easy cleavage. Due to difficulties in crystal growth only the in-plane properties have been reported by Fischer and Brebner (1962), Manfredotti *et al* (1975) and Segura *et al* (1989). The subject has been reviewed by Fivaz and Schmid (1976).

In the present work high quality crystals of InTe and GaTe were grown by the Bridgman technique using very slow growth rates after synthesis from the elements. The crystals were characterized by Laue back reflection and electron diffraction for structure followed by energy dispersive X-ray analysis (EDAX) and X-ray photoelectron spectroscopy (XPS) to establish stoichiometry. Impurity analysis was carried out using inductively coupled plasma emission (ICP). The optical band-gap at 300 K was found to be 1·66 eV and direct in nature. Detailed studies of the electrical transport properties between 10–350°K were thereafter carried out as will be described in this paper. The study of deep levels in orthogonal directions in GaTe has already been reported by Pal *et al* (1994). A new semiconducting ferroelectric has also been found in the related $Ge_{1-x}Ga_xTe$ system by Bose and Pal (1994).

2. Crystal growth

Ga and Te of 6Ns purity were used for synthesis of the compound in sealed quartz

tubes using prolonged and continuous rotation for homogenization. The material was then placed in a conically-tipped ampule in a 3-zone vertical furnace and heated to temperatures well above the melting point of 1097 K. The charge was lowered at 1–1·2 mm/h. A short post-growth anneal at 100–120°C was carried out to give the desired monoclinic phase. The resulting ingots were 1·25 cm in diameter and 2·5 cm in length (Pal *et al* 1994) and could be cleaved easily parallel to the layer planes.

3. Characterization

X-ray powder diffraction studies were carried out which confirmed the monoclinic structure of GaTe with unit cell parameters a = 17·32 A, b = 4·05 A and c = 10·59 A with β = 104·4°. This corresponded to Ga–Ga and Ga–Te bond lengths of 2·473 and 2·638 A respectively and Te–Te distance of 4·096 A. Laue back-reflection showed that the (001) direction was along the layer plane. Electron diffraction studies using a Philips transmission electron microscope (TEM) at 100 keV were also carried out. The diffraction pattern showed the expected 2-fold symmetry and confirmed the values of the lattice parameters. Electron micrographs showed the presence of dislocations in the basal plane and ribbons of stacking faults similar to those in GaSe.

The Ga : Te ratio determined by EDAX and XPS are compared in table 1 which shows reasonable agreement between the bulk and surface.

ICP analysis was conducted on the elements as well as the compound after crystal growth. The principal impurities at trace levels were found to be Pb (0·67 ppm), Sn (0·56 ppm), Fe (0·34 ppm) and Mg (0·26 ppm), the first originating from Ga and the others from Te.

4. Optical absorption

Thin platelets were cleaved from the crystals and polished to mirror finish. The optical absorption was studied perpendicular to the layer plane at 300 K using a UV 365 Shimazu spectrophotometer. The absorption plotted as $(\alpha h\nu)^2$ vs $h\nu$ gave a straight line indicating a direct gap of $1{\cdot}66 \pm 0{\cdot}002$ eV in good agreement with a value of 1·663 eV reported by Brebner and Fischer (1962).

5. Thermoelectric power (TEP)

TEP was measured between 140 and 300 K maintaining a constant temperature

Table 1. Compositional analysis of GaTe single crystals.

	Ga (at %)	Te (at %)
EDAX	49·2–49·3	50·8–50·7
XPS	49·1–49·2	50·9–50·8

difference of 7–8°C between the ends of the samples aligned along or perpendicular to the layer planes. The sign of the TEP was always positive indicating hole conduction. The nature of variation for the two cases is shown in figure 1. At 300 K the TEP in the layer plane was 873 μV/K which increased to 1200 μV/K at 140 K. In the perpendicular direction at 300 K TEP was 1233 μV/K, went through a minimum and thereafter increased to 1550 μV/K at 140 K. The activation energies in two temperature regions given in table 2 were in good agreement with the results of Hall effect measurements. The decrease in TEP with increase in temperature is essentially due to the increase in hole concentration i.e. the Fermi level moves towards the valence band in this temperature range and hence $E_F - E_V$ in (1) decreases.

TEP is related to the Fermi level in a p-type semiconductor by

$$S = +\frac{k}{e}\left[\frac{E_F - E_V}{kT} + A + \frac{5}{2}\right], \quad (1)$$

where A is a constant whose value depends on the scattering mechanism being 3/2, −1/2 or +1/2 for impurity, acoustical phonon or optical phonon scattering respectively. For GaTe along the layer planes between 140–300 K, A = +1/2

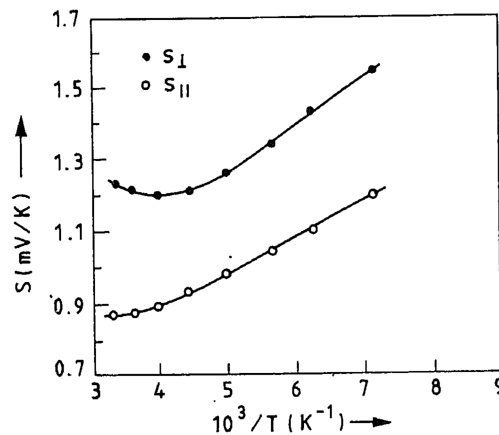

Figure 1. Temperature dependence of thermoelectric power S for p-GaTe parallel and perpendicular to layer plane.

Table 2. Activation energies and hole effective masses in GaTe from TEP studies.

Orientation	E_a (meV) (80–100 K)	E_a (meV) (100–250 K)	m_h^*	A
Parallel to layer plane	22·5	73·6	0·465 m_0 (± 0·01)	+ 0·5
Perpendicular to layer plane	39·7	111·0	0·995 m_0 (± 0·01)	+ 4·5

indicating optical phonon scattering whereas in the perpendicular direction $A = 4{\cdot}5$ in the same temperature range. This cannot be explained by any of the above scattering mechanisms and may be due to the existence of planar defects between the layers. The hole effective masses were calculated from the values of N_V in the two directions and were found to be $0{\cdot}465\,m_0$ and $0{\cdot}995\,m_0$ respectively as given in table 2.

6. Resistivity and Hall effect

The resistivity of samples were measured both along and perpendicular to the layer planes by the van der Pauw method. Ohmic contacts were made by indium evaporation followed by annealing at 200°C in Argon atmosphere for 5 min. Hall effect measurements were carried out between 77–300 K at magnetic fields up to 0·5 T. Arrhenius plots of $\ln\sigma$ and $\ln\sigma$ vs $1/T$ are shown in figure 2. Two sets of activation energies were obtained from the graphs in each direction between 80 and 100 K and 100 and 250 K. The values along the layer planes were 0·023 eV and 0·074 eV respectively lower than the corresponding values 0·040 eV and 0·110 eV in the perpendicular direction. In general $\sigma_{\parallel} \gg \sigma_{\perp}$ as expected for layered compounds the ratio known as the anisotropy factor being given by

$$\sigma_{\parallel}/\sigma_{\perp} = A \exp(\Delta E/kT) = m_{\perp}^{*}/m_{\parallel}^{*} \exp(\Delta E/kT), \quad (2)$$

where $m_{\perp}^{*}$ and $m_{\parallel}^{*}$ are the effective masses. The value of ΔE was found experimentally to be 0·04 eV between 182 and 30 K and shows the effect of defects on $\sigma_{\perp}$.

Figure 3 shows the variation of hole mobility with temperature in the two directions between 80 and 300 K with $p = (2{\cdot}75\text{–}6{\cdot}5) \times 10^{15}/\text{cm}^3$. At 300 K $\mu_{\parallel} = 25-40\,\text{cm}^2/\text{Vsec}$ and $\mu_{\perp} = 10-15\,\text{cm}^2/\text{Vsec}$ while near 80 K these values increased to 450–500 cm^2/Vsec and 100–110 cm^2/Vsec respectively. These are much

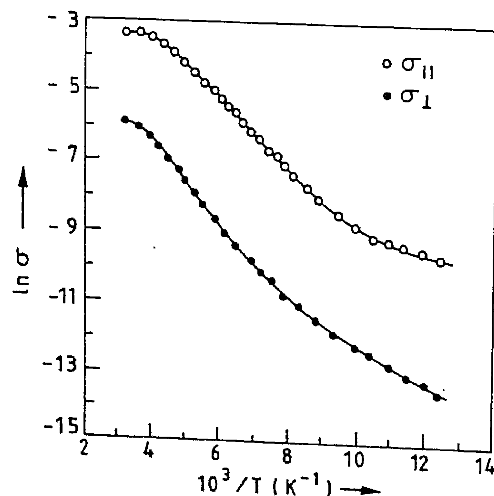

Figure 2. Temperature dependence of conductivity in *p*-GaTe measured parallel and perpendicular to the layer plane.

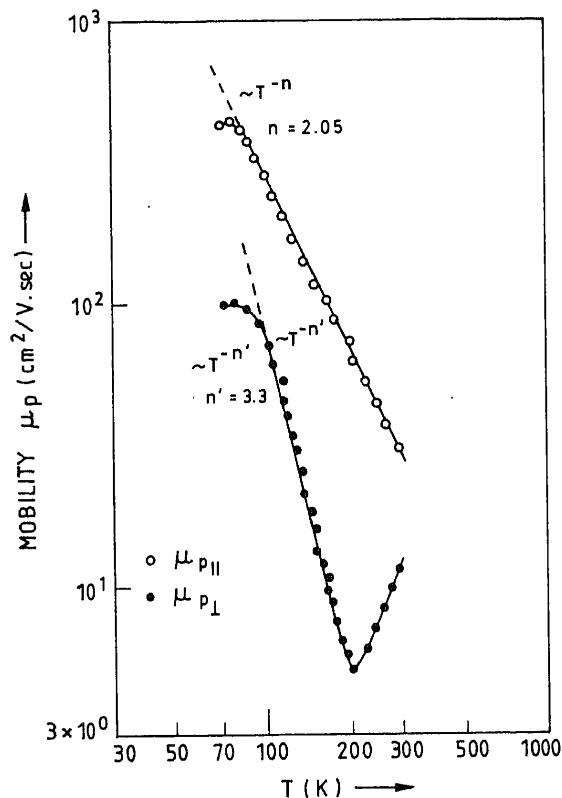

Figure 3. Variation of hole mobility with temperature in two directions (log μ vs log T).

higher than the highest mobility of $\mu_{\parallel}$ = 150 cm^2/Vsec reported by Augelli *et al* (1977) attesting to the high quality of the present crystals. The hole mobility had a temperature dependence for $T > 100$ K given by T^{-n} where n = 2·05 parallel to and 3·3 perpendicular to the layer plane.

The temperature dependence of $\mu_{\parallel}$ has been explained by Fivaz and Schmid (1976) as due to scattering by homopolar optical phonons polarized parallel to the layer planes. Good agreement with this theory was obtained assuming interaction with an optical phonon of energy $\hbar\omega$ = 0·014 eV which was observed in Raman studies by Cerdeira *et al* (1977). If the carrier-lattice coupling constant $g^2 = 0{\cdot}31$ as estimated by Camassel *et al* (1977), the in-plane effective mass m^* = 0·47 m_0 is in excellent agreement with TEP results. The hole density-of-states effective mass was estimated by Manfredotti *et al* (1975) to be 0·6 m_0. From this the effective mass perpendicular to the layer planes is found to be 1·0 m_0, again in good agreement with the value of 0·995 m_0 obtained from TEP (table 2).

The Hall mobility $\mu_{\perp}$ showed a minimum with a thermally activated behaviour for $T > 200$ K with ΔE = 0·040 eV as observed in the case of the conductivity anisotropy. Similar behaviour has been observed in GaSe and is attributed to the presence of interlayer stacking faults.

7. 2D localization studies

Weak localization in InSe has been reported by El-Khatouri *et al* (1989) who examined conductivity variation with temperature but only along the layer planes. Conductivity studies were thus carried out for GaTe between 10–50 K in a closed cycle He cryostat with the electric field parallel or perpendicular to the layer planes. Results are given in figures 4a and b and summed up in table 3.

It is seen (figure 4a) that parallel to the layer plane weak localization occurs for $T < 20$ K the relation followed being given by (Lee and Ramakrishnan 1985),

$$\Delta G = (\lambda e^2/\hbar^2) \ln T, \tag{3}$$

where $\lambda = \alpha p^2/2\pi^2$. From experiment $\lambda = 0{\cdot}051$ giving $p = 1$ for a non-interacting electron gas with $\alpha = 1$. The value of $(e^2/2\pi^2 h)$ was found from the slope to be $1{\cdot}23 \times 10^{-5}$ mhos.

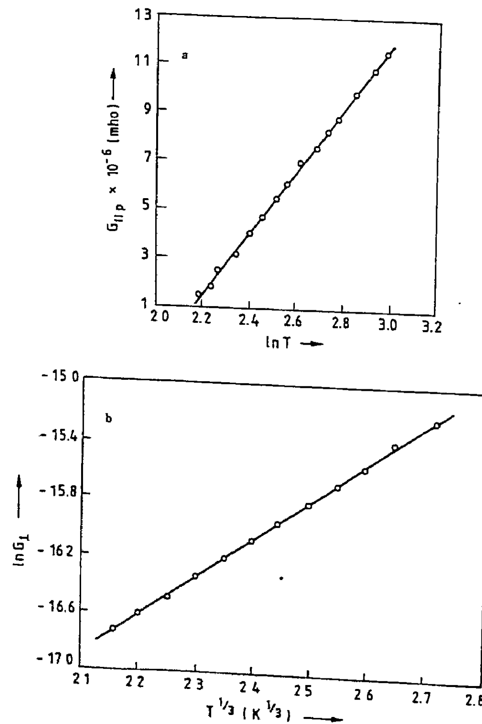

Figure 4. **a.** Conductance G vs ln T along the layer planes for $T = 9$–20 K and **b.** conductance ln G vs $T^{1/3}$ perpendicular to the layer planes for $T = 9$–20 K.

Table 3. Conductivity variation of GaTe in orthogonal directions.

Direction	T = 9–20 K	T = 20–50K
Parallel to layer plane	$G \propto \ln T$	$\sigma \propto T^{1/2}$
Perpendicular to plane	$G \propto \exp(T/T_0)^{1/3}$	$\sigma \propto \exp(T/T_0)^{1/4}$

For $T = 20$–50 K the $T^{1/2}$ variation is a consequence of 3-dimensional conduction under weak localization which is proportional to $T^{p/2}$, where $p = 1$ in the present case.

In the perpendicular direction the temperature variation (figure 4b) is characteristic of 2-D hopping for $T < 20$ K with dimensional crossover to 3-D Mott-type hopping for $T > 20$ K. These results have been discussed in detail by Basak (1994).

The two-dimensional nature of conduction parallel to the layer planes resulted in negative longitudinal magnetoresistance (positive magnetoconductance) being observed at low temperatures with relatively weak fields $< 0{\cdot}4$ T. The results are depicted in figure 5a and summarized in table 4. At 10 K the application of magnetic field results in suppression of weak localization and hence increase in conductance which is proportional to H^2 (figure 5b). At $T = 80$ K for band conduction, increase in scattering and decrease in hole mean-free-path due to the applied magnetic field results in positive magnetoresistance as expected.

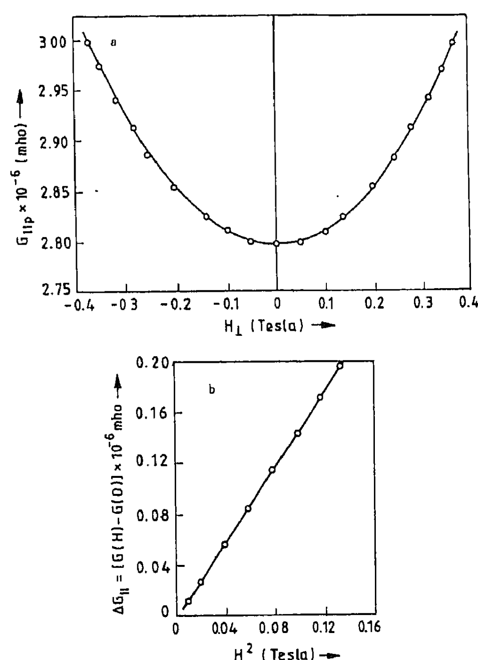

Figure 5. **a.** Transverse magnetoconductance in the layer plane at $T = 10$ K and **b.** change in conductance ΔG vs H^2 at $T = 10$ K.

Table 4. Magnetoresistance in GaTe.

Direction	$(\Delta\rho/\rho)$ (%)	
	$T = 10$ K	$T = 80$ K
Parallel to layers	$-7{\cdot}14\%$	$+ 11{\cdot}5\%$
Perpendicular to layers	$-5{\cdot}18\%$	$+ 8{\cdot}3\%$

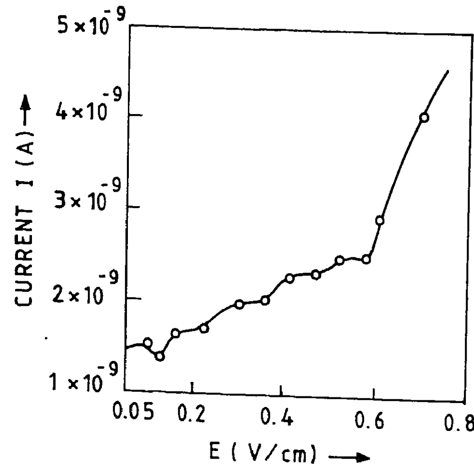

Figure 6. I–V characteristic across the layer plane at $T = 10$ K.

8. I–V characteristics

The I–V characteristics of the samples were studied at 10–25 K at low electric fields both in and across the layer planes. In the latter case it was found that I showed an initial decrease indicating negative differential resistance (NDR) and then increased in discrete steps at 10 K (figure 6), the effect vanishing at 25 K. This behaviour is similar to the resonant tunneling (RT) observed in MBE grown GaAs/$Al_xGa_{1-x}As$ superlattices at 77 K and 300 K by Morkoc *et al* (1986) which also showed NDR. Resonant tunneling of holes, as in the present case, was observed in AlAs/GaAs quantum well structures by Mendez *et al* (1985). RT is due to the applied bias bringing successive quasi-bound states in the narrow regions confined by the potential barriers into alignment permitting tunneling and resulting in the observed current steps. At $T > 20$ K thermal excitation over the potential barriers becomes possible while at higher fields field-assisted tunneling takes over. In the GaAs/AlAs system the confining potential for holes is ~ 150 meV and well widths are typically less than 10 nm which gives large separation between the quantized levels. Hence NDR can be observed at 300 K. For GaTe the confining potentials due to stacking faults are estimated to be a few meV and potential wells are much wider so that the phenomenon is only observed at $T < 10$ K. This is to the authors knowledge the first report of such an observation in a natural superlattice.

9. Conclusion

The study of anisotropy of the transport properties of the layered chalcogenide GaTe revealed novel phenomena which can be explained on the basis of weak localization at low temperatures and its removal due to applied magnetic field resulting in negative magnetoresistance. The anisotropy of effective mass in orthogonal directions was determined from TEP studies while the temperature dependence of mobility μ_H indicated homopolar optical scattering. Resonant tunneling with NDR was observed in such a natural superlattice for the first time.

Acknowledgement

One of the authors (SP) is grateful to the University Grants Commission for the award of a Fellowship.

References

Augelli V, Manfredotti C, Murri R, Piccolo R, Rizzo A and Vasanelli L 1977 *Solid State Commun.* **21** 575

Basak S 1994 *Growth, characterization, electrical and dielectric properties of layered chalcogenides InTe-GaTe*, Ph.D. Dissertation, IIT, Kharagpur

Bose D N and Pal S 1994 *Mater. Res. Bull.* **29** 2, 111

Brebner J L and Fischer G 1962 *Proc. int. conf. phys. semiconductors, Exeter*, (London: Inst. of Phys. & Phys. Soc.) p. 760

Camassel J, Merle P, Mathieu H and Gouskov A 1977 *Phys. Rev.* **B19** 1060

Cerdeira E, Meneses E A and Gouskov A 1977 *Phys. Rev.* **B19** 1648

El-Khatouri D, Khater A, Balkanski M, Julien M and Guesdon J P 1989 *J. Appl. Phys.* **66** 2049

Fischer G and Brebner J L 1962 *J. Phys. Chem. Solids* **23** 1363

Fivaz R C and Schmid P E 1976 *Physics and chemistry of materials with layered structures* (Dordrecht: Reidel) Vol. 4

Lee P A and Ramakrishnan T V 1985 *Rev. Mod. Phys.* **57** 287

Manfredotti C, Murri R, Rizzo A, Vasanelli L and Micocci G 1975 *Phys. Status Solidi* **B65** 249

Mendez A A, Wang W I, Ricco B and Esaki L 1985 *Appl. Phys. Lett.* **47** 415

Morkoc H, Chen J, Reddy U K, Henderson T and Luryi S 1986 *Appl. Phys. Lett.* **49** 70

Pal D, Pal S and Bose D N 1994 *Bull. Mater. Sci.* **17** 347

Segura A, Martinez-Tomas C, Casanovas A, Cantareo A, Martinez-Pastor A and Chevy A 1989 *Appl. Phys.* **A45** 445